

1  
2  
3 1 TITLE: **The sensitivity of US wildfire occurrence to pre-season soil moisture conditions**  
4 2 **across ecosystems**  
5 3

6 4 AUTHORS: Daniel Jensen<sup>1</sup>, John T. Reager<sup>2\*</sup>, Brittany Zajic<sup>1</sup>, Nick Rousseau<sup>1</sup>, Matthew Rodell<sup>3</sup>,  
7 5 and Everett Hinkley<sup>4</sup>  
8 6

9 7 <sup>1</sup>NASA DEVELOP National Program, Science Systems and Applications, Inc.

10 8 <sup>2</sup>NASA Jet Propulsion Laboratory, California Institute of Technology, Pasadena, California, USA

11 9 <sup>3</sup>NASA Goddard Space Flight Center, Greenbelt, Maryland, USA

12 10 <sup>4</sup>National Remote Sensing Program Manager, USDA Forest Service, 1400 Independence Ave.,  
13 11 SW, Washington, DC 20250, USA  
14 12

15 13 \*Correspondence to:

16 14 John T. Reager

17 15 Email: [John.Reager@jpl.nasa.gov](mailto:John.Reager@jpl.nasa.gov)  
18 16  
19 17  
20 18  
21 19  
22 20  
23 21  
24 22  
25 23  
26 24  
27 25  
28 26  
29 27  
30 28  
31 29  
32 30  
33 31  
34 32  
35 33  
36 34  
37 35  
38 36  
39 37  
40 38  
41 39  
42 40  
43  
44  
45  
46  
47  
48  
49  
50  
51  
52  
53  
54  
55  
56  
57  
58  
59  
60

## 41 ABSTRACT

42  
43 It is generally accepted that year-to-year variability in moisture conditions and drought are linked  
44 with increased wildfire occurrence. However, quantifying the sensitivity of wildfire to surface  
45 moisture state at seasonal lead-times has been challenging due to the absence of a long soil  
46 moisture record with the appropriate coverage and spatial resolution for continental-scale analysis.  
47 Here we apply model simulations of surface soil moisture that numerically assimilate observations  
48 from NASA's Gravity Recovery and Climate Experiment (GRACE) mission with the US Forest  
49 Service's historical Fire-Occurrence Database over the contiguous United States. We quantify the  
50 relationships between pre-fire-season soil moisture and subsequent-year wildfire occurrence by  
51 land-cover type and produce annual probable wildfire occurrence and burned area maps at 0.25-  
52 degree resolution. Cross-validated results generally indicate a higher occurrence of smaller fires  
53 when months preceding fire season are wet, while larger fires are more frequent when soils are  
54 dry. This result is consistent with the concept of increased fuel accumulation under wet conditions  
55 in the pre-season. These results demonstrate the fundamental strength of the relationship between  
56 soil moisture and fire activity at long lead-times and are indicative of that relationship's utility for  
57 the future development of national-scale predictive capability.

## 58 59 1. INTRODUCTION

60  
61 Wildfires in the United States have increasingly become larger and more frequent during the last  
62 several decades, contributing to greater environmental degradation, property damage, and  
63 economic losses (Dennison et al. 2014, Morton et al. 2003). By 2025, the cost of fire suppression  
64 in the United States is predicted to increase to nearly \$1.8 billion per year (United States  
65 Department of Agriculture Forest Service 2015). As a result, there is growing need for the  
66 capability to direct operational fire resources before the fire season begins. This points to the  
67 growing importance of seasonal to sub-seasonal forecasting capacity for wildfires, similar to those  
68 that are being developed for weather and natural resources management (National Academies of  
69 Sciences, 2016).

70  
71 Wildfires are typically defined as uncontrolled fires that occur in areas of combustible vegetation,  
72 and depend greatly on vegetation type, structure, arrangement, and moisture. In the contiguous  
73 United States, 90% of wildfire ignitions are associated with human activity, but several other  
74 environmental factors such as fuel availability, fuel moisture, wind, and lightning strikes can be of  
75 critical importance in ignition and growth. The largest contributing factors to general wildfire risk  
76 are the pre-fire-season accumulation of fuels and changing fuel moisture content (FMC), both of  
77 which can contribute to greater fire severity in a given region. Depending on the vegetation class,  
78 more fuels and lower FMC generally indicate higher fire risk and greater fire severity potential—  
79 the degree of environmental change caused by a fire (e.g. Verbesselt et al. 2002; Van Der Werf et  
80 al. 2008).

81

1  
2  
3 82 The spatial distribution and the moisture content of transient (i.e. fast-growing) fuels tend to be  
4 83 associated with precipitation and soil moisture conditions at the land surface over the months prior  
5 84 to fire season, when some regions experience an annual wet period or rainy season (Chuvienco et  
6 85 al. 2004; Krueger et al. 2015). These results suggest that soil moisture may be a good predictor of  
7 86 fire occurrence and fire severity, even at seasonal lead times.  
8  
9

10 87  
11 88 However, in order to understand this relationship, the required local-scale that are adequately  
12 89 discretized and have a spatially and temporally uniform structure are difficult to obtain over large  
13 90 domains (Famiglietti et al. 2008). Therefore it is challenging to develop a quantitative description  
14 91 of the relationship between land surface wetness conditions in the period before fire-season and  
15 92 wildfire occurrence during the fire season, and the specific impacts of surface moisture conditions  
16 93 on wildfire occurrence across land cover types is largely unquantified.  
17 94  
18  
19  
20

21 95 The National Interagency Fire Center currently publishes seasonal fire potential outlook reports  
22 96 for the United States (Predictive Services, National Interagency Fire Center 2016). These reports  
23 97 use the US Drought Monitor, past monthly temperature and precipitation deviations from average,  
24 98 and one and three-month weather outlooks to qualitatively assess regional fire potential. The fire  
25 99 potential maps produced offer a tercile assessment—normal, above normal, or below normal—of  
26 100 fire potential over broad geographic regions. This method does not currently apply a numerical  
27 101 relationship between seasonal fire occurrence and variability in contributing environmental factors  
28 102 such as soil moisture. It also does not yet produce a quantitative estimate of probable fire  
29 103 occurrence that could be used in a risk-assessment framework.  
30  
31  
32  
33

34 104  
35 105 The Palmer Drought Severity Index (PDSI), additionally, has been shown to have utility in  
36 106 assessing drought impacts on wildfire activity (Xiao and Zhuang 2007). However, the PDSI,  
37 107 similar to the National Interagency Fire Center outlook reports, is based on temperature and  
38 108 precipitation sums and not actual soil moisture observations, and has been shown to be biased for  
39 109 assessment of drought conditions in some cases (Sheffield et al. 2012). Burgan et al. (1998) also  
40 110 developed a fire danger fuel model map across different ecoregions, largely based on satellite  
41 111 NDVI observations, but no soil moisture record was then available. These studies provide both a  
42 112 precedent and evidential basis for the use of large-scale climatological variables in wildfire  
43 113 assessment. The recent availability of large-coverage soil moisture products, specifically those  
44 114 produced in a combination of remote sensing and land-surface model simulations through  
45 115 numerical data assimilation, now offer the ability to quantify such relationships at finer scales and  
46 116 across large-domains. The development of these data sets should provide a unique opportunity for  
47 117 advancement in seasonal wildfire risk assessment.  
48  
49  
50  
51  
52

53 118  
54 119 This study thus seeks to integrate NASA earth observation data and the USDA Forest Service's  
55 120 historical fire record to quantify climatic relationships with fire activity. Model-assimilated  
56 121 hydrology observations are leveraged to examine finer spatial and longer temporal scales and to  
57  
58  
59  
60

1  
2  
3 122 establish the quantitative basis for seasonal forecasting relationships. Since pre-season soil  
4 123 moisture can serve as a proxy for pre-season fuel accumulation and live fuel moisture conditions,  
5 124 a historical record of remotely sensed soil moisture data products was examined to disentangle the  
6 125 bearing pre-fire season soil moisture conditions have on a succeeding year's fire activity. With a  
7 126 proven statistical relationship, the methods developed herein can in turn be applied to improve fire  
8 127 prediction and risk assessment capabilities in the contiguous US. As more communities in the earth  
9 128 sciences work at achieving seasonal to sub-seasonal (S2S) predictive capabilities, the importance  
10 129 to society of knowing what might happen at several months lead-time is clear.  
11  
12  
13  
14

15 130  
16 131 Launched in 2002, NASA's Gravity Recovery and Climate Experiment (GRACE) mission  
17 132 provides monthly observations of terrestrial water storage anomalies (TWSA) that describe spatial  
18 133 and temporal changes in the amount of water stored in soils, groundwater and above the land  
19 134 surface (Tapley et al. 2004), which have proven useful in the monitoring of changing hydrologic  
20 135 conditions (e.g. Famiglietti et al. 2011). However, GRACE observations have an intrinsically low  
21 136 spatial resolution ( $\sim 150,000 \text{ km}^2$ ), due to the altitude of the satellites. This makes GRACE TWSA  
22 137 observations difficult to apply for natural resource management. One way to circumvent the  
23 138 resolution limitations of GRACE is to perform a physical downscaling of the GRACE observations  
24 139 through numerical data assimilation. This has been done with much success for drought and flood  
25 140 monitoring applications (Houborg et al. 2012, Reager et al. 2015), and is currently included as an  
26 141 input to the U.S. Drought Monitor framework (Hobourgh et al. 2012). The resulting surface soil  
27 142 moisture data, downscaled from raw GRACE data with the CLSM, form the base climatic  
28 143 independent variable in this study.  
29  
30  
31  
32  
33

34 144  
35 145 Building upon these successes, we investigate the relationship between GRACE-assimilated  
36 146 seasonal surface (top several centimeters) soil moisture (Zaitchick et al. 2008) as a proxy for fuel  
37 147 moisture content and yearly wildfire occurrence and burn extent. We apply GRACE-assimilated  
38 148 soil moisture simulations downscaled with the Catchment Land Surface Model (CLSM) and in-  
39 149 situ wildfire observations over the continental United States during the 2003-2012 period (Short  
40 150 2015), at 0.25-degree spatial resolution, with the 2012-2013 data withheld for validation. Each  
41 151 grid cell represents approximately  $785.18 \text{ km}^2$ , or 194022.02 acres. While other remotely sensed  
42 152 soil moisture data products exist, such as those derived from Soil Moisture and Ocean Salinity  
43 153 (SMOS) and AMSR-E/Aqua, these GRACE-assimilated data offer monthly datasets over a long  
44 154 temporal record and with higher spatial resolution that are more ideal for calibrating a historical  
45 155 regression model over the contiguous United States. We disaggregate the study domain by land  
46 156 cover type (Homer et al. 2015), under the hypothesis that wetness should modulate different land  
47 157 cover responses to wildfire ignition differently. Surface soil moisture alone, as opposed to root  
48 158 zone moisture content and total terrestrial water storage, was utilized in order to optimally capture  
49 159 seasonal variance in wetness that affects all dominant species across land cover types, including  
50 160 grasses with shallow roots (Famiglietti et al. 1999). Additionally, utilizing surface soil moisture in  
51 161 this way provides a reference model that can then be applied with future Soil Moisture Active  
52 162 Passive (SMAP) data. We then determine the historic relationship between wildfire occurrence  
53  
54  
55  
56  
57  
58  
59  
60

1  
2  
3 163 and CLSM-assimilated surface soil moisture across land cover types, and cross-validate a  
4 164 predicted response to show the strength of the relationship. In doing so, this study reveals complex  
5 165 nonlinearities in the influence of fuel moisture content on wildfire severity, and further establishes  
6 166 the need to incorporate accurate surface moisture information in the quantitative assessment of fire  
7 167 risk and potential in the United States. The aim of this study is to demonstrate a relationship  
8 168 between pre-season soil moisture and fire occurrence likelihood and to characterize large-scale  
9 169 fire sensitivity to seasonal moisture patterns.  
10  
11  
12

13 170

## 14 171 2. DATA AND MODELS

15 172

16 173 *2.1 GRACE AND CLSM-DA*

17 174

18 175 NASA's GRACE mission consists of two Earth-observing satellites orbiting in tandem and spaced  
19 176 about 220 kilometers apart at roughly 450 km altitude. A K-band Ranging System (KBR) provides  
20 177 precise measurements (within 10  $\mu\text{m}$ ) of the distance between the satellites caused by spatial and  
21 178 temporal fluctuations in the Earth's gravity field (Tapley et al. 2004). These measurements are  
22 179 used to determine variations in the Earth's mass distribution at a horizontal resolution of 150,000  
23 180  $\text{km}^2$ , with generally higher measurement accuracy across larger spatial scales (Wahr et al. 2004).  
24 181 The monthly to decadal temporal changes in the gravity field are attributed primarily to mass  
25 182 redistribution in the atmosphere, ocean, continents and solid earth. After isolation and correction  
26 183 of 'unwanted' signals for hydrology applications (i.e. ocean, atmosphere, and postglacial rebound),  
27 184 these measurements, referred to as terrestrial water storage anomalies (TWSA), are assumed to  
28 185 approximate the movement of water mass over time. Swenson and Wahr (2004) and Wahr et al.  
29 186 (1998) offer general post-processing logistics and Landerer and Swenson (2012) offer specifics on  
30 187 scaling, signal restoration, and regional error calculation. The GRACE dataset utilized for this  
31 188 project is processed by the Texas Center for Space Research (CSR; version CSR-RL05) and  
32 189 NASA's Jet Propulsion Laboratory. It is a global, monthly, one degree gridded, scaled GRACE  
33 190 land data product available for download at [grace.jpl.nasa.gov](http://grace.jpl.nasa.gov). The data for this project is from  
34 191 the time period April 2002 to December 2013.  
35  
36  
37  
38  
39  
40  
41  
42

43 192

44 193 Developed at the NASA Goddard Space Flight Center, The Catchment Land Surface Model  
45 194 (CLSM) is a physically based land surface model (Koster et al. 2000). For the model forcing, the  
46 195 horizontal structure of a rectangular atmospheric grid is separated into topographically-defined  
47 196 catchments with an estimated average area of 4000  $\text{km}^2$ . Water is spatially and vertically  
48 197 distributed in the model determined by topography and the model's hydrologic processes are  
49 198 generally determined by the catchment's topographical statistics. In the assimilation algorithm, the  
50 199 model-generated terrestrial water storage moisture elements are corrected with the GRACE  
51 200 observational estimate using an Ensemble Kalman Smoothing Filter method (EnKS) as described  
52 201 in Zaitchik et al. (2008). Assimilation incorporates the relative uncertainty in the model and the  
53 202 observations. In this process, a two-step smoother is applied to manage GRACE's monthly  
54 203 temporal resolution both forward and backwards in time. In order to create consistency among  
55  
56  
57  
58  
59  
60

1  
2  
3 204 observed and modeled variables, the GRACE water storage anomalies are changed to absolute  
4 205 values by adding the simulated time mean water storage variable from the CLSM output to the  
5 206 observations. The observations are directly applied to the column-integrated forecasted variable  
6 207 (the catchment deficit) and the primary non-equilibrium prognostic (the root zone excess  
7 208 moisture), and the vertical disaggregation occurs based on covariance. The CLSM-Data  
8 209 Assimilation (CLSM-DA) data used in this study extend from January 2003 to December 2014,  
9 210 and the outputs are reported on 0.25-degree grid cells for the contiguous United States. The gridded  
10 211 analysis used in this paper is an interpolation of catchment tiles to an equally spaced model grid  
11 212 for consistency with the other data sets used. Resampling these other datasets to the coarser  
12 213 resolution always introduces uncertainty but captures more first order climatic characteristics.  
13 214

## 14 215 *2.2 FIRE PROGRAM ANALYSIS-FIRE OCCURRENCE DATABASE*

15 216

16 217 The USDA Forest Service's Fire Program Analysis Fire-Occurrence database (FPA FOD) is a  
17 218 comprehensive geospatial database of wildfires in the United States from 1992 to 2013. It includes  
18 219 1.73 million geo-referenced wildfire records, representing a total of 126 million acres burned  
19 220 during the 22-year period (Short 2015). It also contains vital information for each of these fires,  
20 221 including date, cause, fire size, fire class, burned area, and coordinates. These data were imported  
21 222 as points into a geographic information system and processed into two separate raster datasets that  
22 223 matched the spatial and temporal resolution of the GRACE derived soil moisture data. The first  
23 224 dataset aggregated the annual number of fires in each  $0.25 \times 0.25$  degree cell for May through  
24 225 April of the following year, while the second summed the total burned area (in acres) for each cell  
25 226 in that timeframe.  
26 227

## 27 228 *2.3 NATIONAL LAND COVER DATABASE*

28 229

29 230 The land cover type dataset used in this study was the USGS' National Land Cover Database 2011  
30 231 (NLCD 2011) (Homer et al. 2015). This dataset maps land cover and land use across the United  
31 232 States at a 30 meter resolution. The NLCD data were first reclassified for generalization and  
32 233 resampled to the same spatial extent and resolution as the previous two datasets using a majority  
33 234 resampling technique that allocates each pixel's class based on the most popular value within a 3  
34 235 by 3 window. This allowed each grid cell to have a unique land cover classifier, which could then  
35 236 be programmatically used to extract values and characterize each relevant vegetation type's  
36 237 relationship between soil moisture and wildfire. For the purposes of this study, only vegetated land  
37 238 cover types are of importance to wildfires. Accordingly, the Developed/Urban, Barren Land, and  
38 239 Planted/Cultivated classes were not considered in the analysis. The Mixed Forest class was not  
39 240 considered due to its unsuitably small number of pixels. Additionally, even though model  
40 241 simulations of wetland soil moisture may not be accurate due to missing physical processes, we  
41 242 include this class to represent general wet/dry responses in wetland environments. Figure 1 shows  
42 243 a visualization of this processed land cover data along with the other two datasets mentioned above.  
43 244  
44  
45  
46  
47  
48  
49  
50  
51  
52  
53  
54  
55  
56  
57  
58  
59  
60

### 245 3. METHODS

246

#### 247 3.1 DATA PROCESSING

248

249 The first step in algorithm development was to disaggregate the fire data by wildfire size class  
250 (Table 1). Annual January through April (2003-2014) soil moisture from the GRACE-derived  
251 CLSM-DA data were averaged into single two-dimensional maps (latitude  $\times$  longitude) for each  
252 year that depict a fire season's antecedent moisture conditions (Xystrakis et al. 2014). Annual total  
253 fire occurrence and cumulative burned area maps, aggregated from the rasterized FPA FOD data,  
254 were produced for each wildfire class, covering the period ranging May through April of the  
255 following year. This time period was selected in order to delineate a nominal fire season in line  
256 with the beginning of the Western US fire season, although true fire season tends to vary in time  
257 and by location (Westerling et al. 2003). Within each land cover type, all burned area and fire  
258 occurrence values—which here refers to the total number of fires occurring in a given grid cell—  
259 were plotted against corresponding CLSM-DA soil moisture values for the entire population of  
260 0.25-degree grid cells. While wildfires belonging to a smaller size class constitute only a fraction  
261 of a percent of their parent grid cell, the frequency of their occurrence within each discretized area  
262 is an important climatological figure linking soil moisture to fire activity.

263

264 This produced a distribution of fire occurrence, visible in Figure 1, and burned area as a function  
265 of soil moisture for each land cover class. These data were then binned by soil moisture ranges to  
266 calculate average fire occurrence and burned area values over each range. These distributions  
267 reveal the unique relationship in each land cover class between occurrence of wildfires of  
268 increasing size classification as a function of soil moisture state. These relationships were then  
269 individually modeled by fitting an exponential or linear function depending on which resulted in  
270 a higher  $R^2$  value. If neither function's  $R^2$  surpassed 0.5, meaning pre-season soil moisture explains  
271 less than 50% of the variance in fire activity, mean number of fires and mean burned area were  
272 plotted instead. This methodology is displayed for fire occurrence in Figure 2 for each land cover  
273 type and fire size class, and the same method was followed for burned area.

274

275 We also investigated whether the information contained in these relationships with soil moisture  
276 demonstrated predictive utility. Comprehensive deterministic prediction is challenging, because  
277 we don't include all of the information required to determine the comprehensive source and forcing  
278 for all fire occurrence and severity; variables such as lightning strikes, human activity, wind gusts,  
279 and fuel loading all contribute substantially to actual wildfire predictability. Instead, we investigate  
280 a statistical tendency of soil moisture to affect wildfire occurrence by lumping a large population  
281 of observations into a single model, and evaluating how the population responds as whole to this  
282 single factor. We assume that the population captures the probable best estimate of the relationship  
283 that would occur at a single location under different conditions and across time. A comprehensive  
284 fire prediction model could likely include other forcing variables.

285

286

287

288

289

290

### 286 3.2 PREDICTIVE MODEL

287  
288 Each modeled distribution's fitted function or mean was referenced for mapping fire probability  
289 and predicted burned area. Fire probability and average burned area were calculated by applying  
290 each individual pre-season soil moisture value to the function corresponding to its land cover type  
291 for the relevant fire size class. Probable total burned area (Equation 1) is then estimated by  
292 multiplying the modeled fire occurrence by the modeled average burned area value for each cell's  
293 soil moisture value as broken down by land cover type and fire size class.

$$294$$
$$295 \text{ Probable Burned Area}(i) = \text{Fire Occurrence}(SM_i, LC_i) \times \text{Average Burned Area}(SM_i, LC_i)$$
$$296 \quad (1)$$

297  
298 In Equation 1,  $i$  is a given 0.25 degree grid cell, and  $SM_i$  and  $LC_i$  are the corresponding values of  
299 soil moisture and land cover classification. Maps for both predicted number of fires and predicted  
300 burned area were thus created for each fire size class. These maps, binned by fire size for each  
301 parameter, can be added together to create maps for a year's total predicted number of fires and  
302 total burned acreage.

## 303 4. RESULTS

304  
305  
306 Figure 2 shows that within each land cover type, there are different distributions of fire occurrence  
307 as a function of soil moisture for each fire class. For example, within the evergreen forest type, the  
308 smaller fire classes B, C, and D tend to be more frequently associated with a higher average number  
309 of fires following high pre-fire season soil moisture. Meanwhile, the larger fire classes E, F, and  
310 G, show the opposite trend whereby dryer soil moisture conditions in January – April are  
311 associated with more fires throughout the following year. Some distributions are relatively uniform  
312 and showing little variability. This indicates the absence of a clear relationship between soil  
313 moisture and fire occurrence, or that other factors tend to mask that relationship. Each vegetation  
314 type differs from the other in its surface soil moisture and fire occurrence and size patterns.  
315 Deciduous forest tends to be the wettest modeled ecosystem (mean volumetric water content  
316 fraction = 0.31, standard deviation = 0.06) and shrubland tends to be the driest (mean volumetric  
317 water content fraction = 0.19, standard deviation = 0.05). Wetland ecosystems have the most fires  
318 per cell on average (11.46 fires per year, standard deviation = 16.79), while shrublands have the  
319 fewest (3.48 fires per year, standard deviation = 9.16). These values were calculated by compiling  
320 the pre-season surface soil moisture and fire occurrence values across all cells within each land  
321 cover type for each year in the study period. These values indicate the need to disaggregate the  
322 relationship between fire occurrence and soil moisture by land cover type, as each type shows a  
323 significantly different fire response to soil moisture levels.

324  
325 Figure 3 provides an example of results by hindcasting the May 2012 – April 2013 fire year. The  
326 top map shows the total number of fires expected to occur in each cell that year based on the



1  
2  
3 327 preceding January – April average soil moisture. Figure 3 (bottom) shows total predicted burned  
4 328 acreage. The spatial gaps in the predictive maps represent the withheld land cover classes. These  
5 329 maps were created for each year in the study period, and their summary statistics for predicted  
6 330 number of fires and total burned acres were compiled and charted in Table 2 and Figure 4.  
7  
8  
9 331

10 332 To validate these results, predicted fire occurrence and burned area maps that were generated for  
11 333 the 2012 – 2013 fire year (i.e. the most recent year in the FPA FOD dataset), and compared against  
12 334 the observations. For proper cross-validation, this fire year was held out of the algorithmic step.  
13 335 Results are compiled in Table 2. Additionally, the processed FPA FOD data was disaggregated by  
14 336 land cover type and charted next to the predicted fire data, as shown for May 2012 – April 2013  
15 337 in Figure 4, showing the relative accuracy of the algorithm’s prediction for each vegetation type  
16 338 with standard percent error calculations (Equation 2).  
17  
18  
19 339

$$20 \quad 340 \quad \%_{error} = \left| \frac{\#_{experimental} - \#_{theoretical}}{\#_{theoretical}} \right| \times 100 \quad (2)$$

21 341  
22  
23 342 Vegetation types that were deemed unsuitable for the analysis (i.e. mixed forest, agricultural, and  
24 343 urban) were removed from the data sets. Figure 4 shows that in the 2012 – 2013 case study, the  
25 344 values for predicted fire occurrence and burned area match the actual data within an error of  
26 345 13.89% and 9.52% respectively, compared to an average error 13.10% for predicted fires and  
27 346 119.40% for predicted burned area for the entire study period.  
28  
29  
30 347

## 31 348 5. DISCUSSION AND CONCLUSIONS

32 349  
33  
34 350 It should be noted that the predictive maps presented are not intended to offer an accurate hindcast  
35 351 of actual fire occurrence and severity in individual 0.25-degree grid cells. Rather, they offer an  
36 352 assessment of the relationship between seasonal soil moisture and wildfire potential, specifically  
37 353 the sensitivity of fires in the fire season to pre-season surface moisture conditions. The modeled  
38 354 functions and validation results show that the total number of fires and burned area predicted is in  
39 355 fact correlated with the pre-season soil moisture data for the corresponding year, across the land  
40 356 cover grouping. A positive correlation would indicate that high pre-season soil moisture is  
41 357 followed by high fire activity, while a negative correlation would see low fire activity. Regional  
42 358 hindcasting of fire occurrence was performed by aggregating the land-cover consistent regions in  
43 359 their entirety over the contiguous US, and optimizing the fire response model for each land cover  
44 360 type. This improves upon an ecoregion approach for which a number of included land cover types  
45 361 may exist, and a corresponding number of fire responses to moisture may occur (e.g. Parks et al.  
46 362 2014). The strong correlation achieved in our results highlights the principal importance of  
47 363 pre-season soil moisture in governing fire risk and potential, likely as a proxy for pre-season fuel  
48 364 accumulation.  
49  
50  
51  
52  
53  
54  
55 365

56 365

1  
2  
3 366 These results provide the first evidence that pre-season soil moisture and wildfire occurrence can  
4 367 be strongly negatively correlated across land cover types. In all land covers, the smaller fire classes  
5 368 (i.e. class “D” or smaller, <300 acres) are generally (11 out of 20 scenarios) associated with higher  
6 369 pre-season soil moisture, not lower soil moisture as hypothesized. This likely describes a situation  
7 370 in which smaller and quick-growing vegetation (e.g. grasses and understory) are more prolific in  
8 371 wet years, and tend to contribute to wildfire persistence and propagation after ignition. As the  
9 372 resampled NLCD 2011 data was implemented in our algorithm, land cover is assumed to be static  
10 373 over the study period. It is possible that this represents an additional error source in our regression,  
11 374 though there is no clear pattern in the percent error figures (Table 2) and land cover changes may  
12 375 represent a small fraction of the regressed relationships across the entire aggregated domain. The  
13 376 random error structure suggests that the model error is more associated with year-to-year weather  
14 377 and soil moisture patterns rather than land-cover change. As soil moisture in this study is used as  
15 378 a proxy for vegetation moisture and general climate conditions, a wet pre-season in certain  
16 379 vegetation types is correlated with more primary production creating increased fuel availability  
17 380 when fire season arrives. This is further corroborated by observations made by Xystrakis et al.  
18 381 (2014), which saw high spring precipitation succeeded by high burned area values. The case that  
19 382 would lead to the most fires in these land cover types is likely that of a very wet pre-season,  
20 383 followed by a very dry fire season. This relationship has been studied before using precipitation  
21 384 observations (e.g. Holden et al. 2007).

22 385  
23 386 While the necessity is clear, the feasibility of wildfire predictive capabilities is increasing with the  
24 387 advent of innovative applications of new remote sensing data. As our analysis focused on  
25 388 quantifying and validating the overall relationship between pre-season soil moisture and  
26 389 succeeding fire activity rather than providing accurate annual fire activity predictions, model  
27 390 outputs are not intended to be applied as accurate annual fire activity predictions. While the model  
28 391 illuminates this relationship, its performance may be negatively affected by limitations in the  
29 392 datasets and omitted environmental factors. For one, resampling the NLCD land cover to the  
30 393 coarser GRACE-DA resolution inevitably decreased the purity of each pixel’s designated land  
31 394 cover type. Using finer-scale SMAP data to expand this analysis may mitigate these effects, and  
32 395 additionally improve the retrieval of burned area. Since accurate, observation-based surface soil  
33 396 moisture information has been difficult to obtain over large domains, GRACE-assimilated model  
34 397 outputs may offer a unique contribution to fire severity prediction methods. This builds upon  
35 398 successes in using GRACE-assimilated model outputs for hydrologic drought monitoring  
36 399 (Houborg et al. 2012), and reinforces the importance of the relationship between large-scale  
37 400 hydrologic forcing and fire response. The current NASA SMAP mission (Entekhabi et al. 2010),  
38 401 launched January, 2015, offers global observations of radiometer-based surface soil moisture at a  
39 402 base 36-km spatial resolution that can be used in conjunction with GRACE-assimilation efforts  
40 403 and should generally improve this methodology. The expanding temporal and spatial coverage of  
41 404 soil moisture brought about by SMAP will additionally allow this methodology to be applied in  
42 405 regions with more heterogeneous land cover conditions due to higher resolutions. These more  
43 406 complex regions may also be approached with regionally sensitive environmental parameters to

1  
2  
3 407 generate more accurate regional predictive fire maps. For example, the classification of large  
4 408 swaths of Minnesota and Michigan as wetland in the NLCD (Figure 1) caused those areas' fire  
5 409 frequency to be greatly overestimated as a result of the high fire activity in Florida's Everglades  
6 410 and other wetland regions (Figure 3). Indeed, the wetland regression models (Figure 2) do not  
7 411 show high correlation coefficients except in the case of large fires, indicating regional processes  
8 412 controlling the majority of the variance. Other regional drivers of fire activity that see great spatial  
9 413 and temporal variability, such as fuel moisture, wind, and lightning patterns may (Veraverbeke et  
10 414 al. 2017) may further reduce the modeled discrepancies in fire occurrence and intensity. Along  
11 415 with the finer-scale SMAP data, the fundamental relationship between soil-moisture and fire  
12 416 activity observed in this study could be built upon using other environmental variables to generate  
13 417 monthly regional predictive fire maps.  
14  
15  
16  
17  
18

## 19 418 20 419 6. ACKNOWLEDGMENTS

21 420  
22 421 This research was conducted at the Jet Propulsion Laboratory, California Institute of Technology,  
23 422 under contract with NASA. We would like to thank Mark Finney and Chuck McHugh, from the  
24 423 USDA Forest Service Predictive Services Program for their involvement in providing direction  
25 424 and information pertaining to wildfires in the United States. This work was supported by the  
26 425 NASA DEVELOP program, through contract NNL11AA00B and cooperative agreement  
27 426 NNX14AB60A. Funding sources include the NASA Applied Sciences Program and the NASA  
28 427 GRACE Science Team. The data supporting this study's conclusions consist of the included tables  
29 428 and figures. The FPA FOD data (Short, 2015) can be accessed at [http://dx.doi.org/10.2737/RDS-](http://dx.doi.org/10.2737/RDS-2013-0009.3)  
30 429 2013-0009.3. The assimilated GRACE data is available at <http://grace.jpl.nasa.gov>. The NLCD  
31 430 2011 is available at <http://www.mrlc.gov/nlcd2011.php>.  
32  
33  
34  
35  
36

## 37 431 38 432 7. REFERENCES

- 39 433  
40 434 Burgan, R., Klaver, R., & Klaver, J. (1998). Fuel Models and Fire Potential From Satellite and  
41 435 Surface Observations. *International Journal of Wildland Fire*, 8(3), 159.  
42 436 <https://doi.org/10.1071/WF9980159>  
43 437 Chuvieco, E., I. Aguado, and A. P. Dimitrakopoulos (2004), Conversion of fuel moisture content  
44 438 values to ignition potential for integrated fire danger assessment, *Can. J. For. Res.*, 34(11),  
45 439 2284–2293, doi:10.1139/x04-101.  
46 440 Dennison, P. E., S. C. Brewer, J. D. Arnold, and M. A. Moritz (2014), Large wildfire trends in  
47 441 the western United States, 1984-2011, *Geophys. Res. Lett.*, 41, 2928–2933,  
48 442 doi:10.1002/2013GL058954.  
49 443 Entekhabi, D. et al. (2010), The soil moisture active passive (SMAP) mission, *Proc. IEEE*, 98(5),  
50 444 704–716, doi:10.1109/JPROC.2010.2043918.  
51 445 Famiglietti, J., J. Devereaux, C. Laymon, T. Tsegaye, P. Houser, T. Jackson, S. Graham, M.  
52 446 Rodell, and P. van Oevelen (1999), Ground-based investigation of soil moisture variability  
53 447 within remote sensing footprints during the Southern Great Plains 1997(SGP97) Hydrology  
54 448 Experiment, *Water Resources Research*, 35(6), 1839–1851.  
55 449 Famiglietti, J. S., Ryu, D., Berg, A. A., Rodell, M., & Jackson, T. J. (2008). Field observations of  
56  
57  
58  
59  
60

- 1  
2  
3 450 soil moisture variability across scales. *Water Resources Research*, 44(1).  
4 451 <http://doi.org/10.1029/2006WR005804>  
5  
6 452 Homer, C.G., J.A. Dewitz, L. Yang, S. Jin, P. Danielson, G. Xian, J. Coulston, N.D. Herold, J.D.  
7 453 Wickham, and K. Megown (2015), Completion of the 2011 National Land Cover Database  
8 454 for the conterminous United States-Representing a decade of land cover change  
9 455 information. *Photogrammetric Engineering and Remote Sensing* 81(5), 345-354.  
10 456 Houborg, R., M. Rodell, B. Li, R. Reichle, and B. F. Zaitchik (2012), Drought indicators based  
11 457 on model-assimilated Gravity Recovery and Climate Experiment (GRACE) terrestrial water  
12 458 storage observations, *Water Resour. Res.*, 48(July), doi:10.1029/2011WR011291.  
13 459 Koster, R. D., M. J. Suarez, A. Ducharne, M. Stieglitz, and P. Kumar (2000), A catchment-based  
14 460 approach to modeling land surface processes in a general circulation model: 1. Model  
15 461 structure, *J. Geophys. Res.*, 105(D20), 24809–24822.  
16 462 Krueger, E. S., T. E. Ochsner, D. M. Engle, J. D. Carlson, D. Twidwell, and S. D. Fuhlendorf  
17 463 (2015), Soil Moisture Affects Growing-Season Wildfire Size in the Southern Great Plains,  
18 464 *Soil Sci. Soc. Am. J.*, 79(6), 1567–1576, doi:10.2136/sssaj2015.01.0041.  
19 465 Landerer, F. W., and S. C. Swenson (2012), Accuracy of scaled GRACE terrestrial water storage  
20 466 estimates, *Water Resour. Res.*, 48(4), 1–11, doi:10.1029/2011WR011453.  
21 467 Morton, D. C., M. E. Roessing, A. E. Camp, and M. L. Tyrrell (2003), *Assessing the*  
22 468 *Environmental, Social, and Economic Impacts of Wildfire*, New Haven, CT.  
23 469 National Academies of Sciences, Engineering, and Medicine (2016) *Next Generation Earth*  
24 470 *System Prediction: Strategies for Subseasonal to Seasonal Forecasts*. Washington, DC: The  
25 471 National Academies Press. doi:<https://doi.org/10.17226/21873>.  
26 472 National Significant Wildland Fire Potential Outlook. (2016). Predictive Services, National  
27 473 Interagency Fire Center. Boise, Idaho. Retrieved from  
28 474 <http://www.predictiveservices.nifc.gov/outlooks/outlooks.htm>  
29 475 Reager, J., Thomas, A., Sproles, E., Rodell, M., Beaudoin, H., Li, B., & Famiglietti, J. (2015).  
30 476 Assimilation of GRACE Terrestrial Water Storage Observations into a Land Surface Model  
31 477 for the Assessment of Regional Flood Potential. *Remote Sensing*, 7(11), 14663–14679.  
32 478 <http://doi.org/10.3390/rs71114663>  
33 479 Rodell, M. (2013), "Application of satellite gravimetry for water resource vulnerability  
34 480 assessment", chapter in *Climate Vulnerability: Understanding and Addressing Threats to*  
35 481 *Essential Resources*, Elsevier Inc., Academic press, pp. 151-159.  
36 482 Short, Karen C. (2015). Spatial wildfire occurrence data for the United States, 1992-2013  
37 483 (FPA\_FOD\_20150323). 3rd Edition. Fort Collins, CO: Forest Service Research Data  
38 484 Archive. <http://dx.doi.org/10.2737/RDS-2013-0009.3>.  
39 485 Swenson, S., and J. Wahr (2006), Post-processing removal of correlated errors in GRACE data,  
40 486 *Geophys. Res. Lett.*, 33(8), doi:10.1029/2005GL025285.  
41 487 Tapley, B. D., S. Bettadpur, J. C. Ries, P. F. Thompson, and M. M. Watkins (2004), GRACE  
42 488 measurements of mass variability in the Earth system., *Science* (80-. ), 305, 503–505,  
43 489 doi:10.1126/science.1099192.  
44 490 The Rising Cost of Fire Operations: Effects on the Forest Service's Non-Fire Work. (2015).  
45 491 United States Department of Agriculture Forest Service. Retrieved from  
46 492 <http://www.fs.fed.us/sites/default/files/media/2014/34/nr-firecostimpact-082014.pdf>  
47 493 Van Der Werf, G. R., J. T. Randerson, L. Giglio, N. Gobron, and a. J. Dolman (2008), Climate  
48 494 controls on the variability of fires in the tropics and subtropics, *Global Biogeochem. Cycles*,  
49 495 22, 1–13, doi:10.1029/2007GB003122.  
50  
51  
52  
53  
54  
55  
56  
57  
58  
59  
60

- 1  
2  
3 496 Veraverbeke, S., B. M. Rogers, M. L. Goulden, R. R. Jandt, C. E. Miller, E. B. Wiggins, and J.  
4 497 T. Randerson. 2017. Lightning as a Major Driver of Recent Large Fire Years in North  
5 498 American Boreal Forests. *Nature Climate Change* 7 (7): 529–34.  
6 499 doi:10.1038/nclimate3329.  
7  
8 500 Verbesselt, J., S. Fleck, and P. Coppin (2002), Estimation of fuel moisture content towards fire  
9 501 risk assessment: a review, in *Proceedings of the 6th International Conference on Forest*  
10 502 *Fire Research*.  
11  
12 503 Wahr, J., M. Molenaar, and F. Bryan (1998), Time variability of the Earth's gravity field:  
13 504 Hydrological and oceanic effects and their possible detection using GRACE, *J. Geophys.*  
14 505 *Res.*, 103(B12), 205–229.  
15  
16 506 Wahr, J., S. Swenson, V. Zlotnicki, and I. Velicogna (2004), Time-variable gravity from  
17 507 GRACE: First results, *Geophys. Res. Lett.*, 31(11), doi:10.1029/2004GL019779.  
18 508 Westerling, A. L., A. Gershunov, T. J. Brown, D. R. Cayan, and M. D. Dettinger (2003), Climate  
19 509 and wildfire in the western United States, *Bull. Am. Meteorol. Soc.*, 84(5), 595–604,  
20 510 doi:10.1175/BAMS-84-5-595.  
21 511 Xiao, J. F., & Zhuang, Q. L. (2007). Drought effects on large fire activity in Canadian and  
22 512 Alaskan forests. *Environmental Research Letters*, 2(4), 44003. [https://doi.org/Artn](https://doi.org/Artn044003)  
23 513 [044003](https://doi.org/10.1088/1748-9326/2/4/044003)\rDoi 10.1088/1748-9326/2/4/044003  
24  
25 514 Xystrakis, F., Kallimanis, A. S., Dimopoulos, P., Halley, J. M., & Koutsias, N. (2014).  
26 515 Precipitation dominates fire occurrence in Greece (1900-2010): Its dual role in fuel build-up  
27 516 and dryness. *Natural Hazards and Earth System Sciences*, 14(1), 21–32.  
28 517 <https://doi.org/10.5194/nhess-14-21-2014>  
29  
30 518 Zaitchik, B. F., M. Rodell, and R. H. Reichle (2008), Assimilation of GRACE Terrestrial Water  
31 519 Storage Data into a Land Surface Model: Results for the Mississippi River Basin, *J.*  
32 520 *Hydrometeorol.*, 9, 535–548, doi:10.1175/2007JHM951.1.  
33  
34  
35  
36  
37  
38  
39  
40  
41  
42  
43  
44  
45  
46  
47  
48  
49  
50  
51  
52  
53  
54  
55  
56  
57  
58  
59  
60

## 521 8. TABLES

522

523 **Table 1.** Fire Size Class Definitions<sup>1</sup>

<b>Class</b>	<b>Burned Acres</b>
A	0 – 0.25
B	0.26 – 9.9
C	10 – 99.9
D	100 – 299
E	300 – 999
F	1000 – 4999
G	5000 +

524 <sup>1</sup>Class size ranges are defined by (Short 2015)

525

526

527 **Table 2.** Predicted and Actual Fire Data with Associated Prediction Errors

	<b>Predicted Fires</b>	<b>Actual Fires</b>	<b>Predicted Burned Acres</b>	<b>Actual Burned Acres</b>	<b>Predicted Fires Percent Error</b>	<b>Predicted Burned Area Percent Error</b>
5/2003 - 4/2004	59410	53542	7356289.94	3333260.32	10.96	120.69
5/2004 - 4/2005	58131	44304	7429770.21	1288883.79	31.21	476.45
5/2005 - 4/2006	61526	72461	7472239.08	6710199.52	11.36	15.09
5/2006 - 4/2007	56998	66903	7343697.15	7181219.66	2.26	14.81
5/2007 - 4/2008	57954	62238	7427601.87	8680825.32	6.88	14.44
5/2008 - 4/2009	56177	59937	7357446.45	3887901.30	6.27	89.24
5/2009 - 4/2010	56337	43507	7407664.38	1603893.48	29.49	361.86
5/2010 - 4/2011	61071	55468	7510430.96	4935915.82	10.10	52.16
5/2011 - 4/2012	57448	52897	7423439.20	5312742.66	8.60	39.73
5/2012 - 4/2013	55442	48679	7559133.21	8354888.73	13.89	9.52

528

529

530

531

532

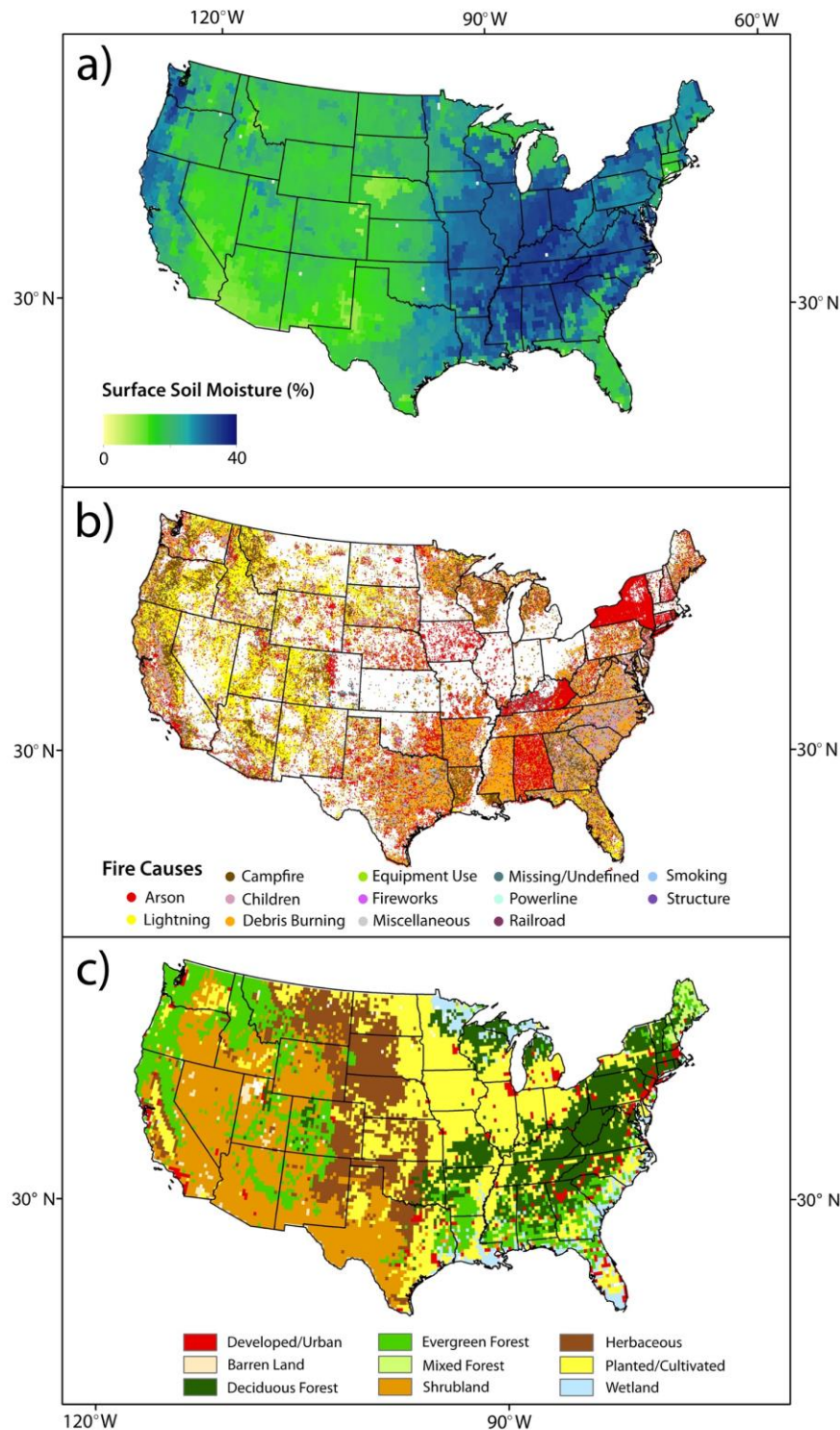
533

58

59

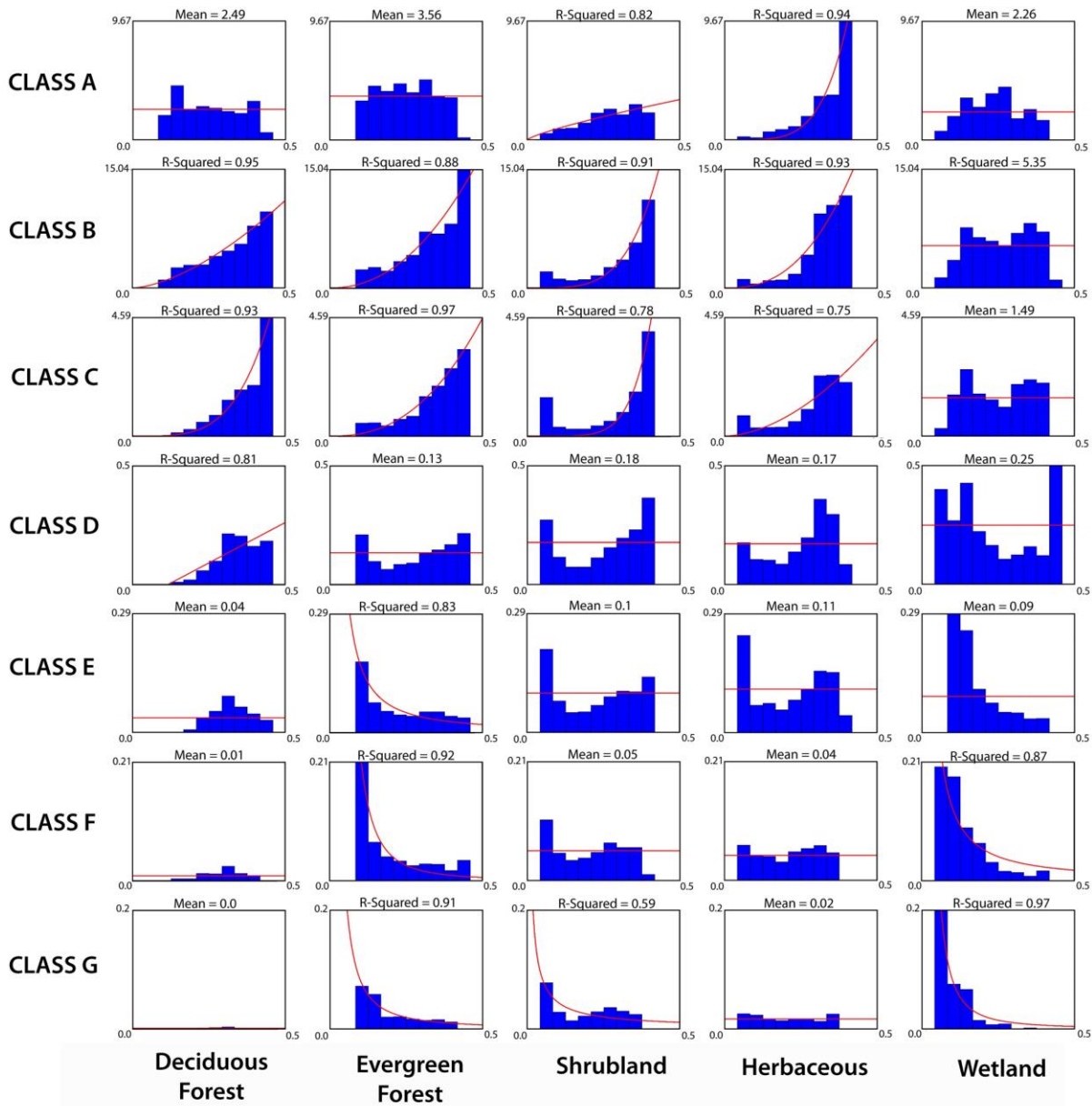
60

## 534 9. FIGURES



535  
 536 **Figure 1.** The datasets used in this study: (a) GRACE-derived volumetric surface soil moisture  
 537 expressed as percent. This example shows average January – April surface soil moisture from 2003  
 538 – 2013. (b) All fires from the 2003 – 2013 study period in the FPA FOD mapped as points by fire  
 539 cause. (c) The NLCD 2011 resampled to a 0.25-degree resolution.

540



541

542

543

544

545

546

547

548

**Figure 2.** Binned average fire occurrence over each complete year and associated fitted functions or mean values for each analyzed land cover type by fire size class. The x-axis of each chart denotes surface soil moisture as a percentage, and the y-axis shows the average number of fires per 0.25 degree cell for that soil moisture bin. The fire size classes are defined by Short (2015), displayed in Table 1.

549

550

551

552

553

554

555

556

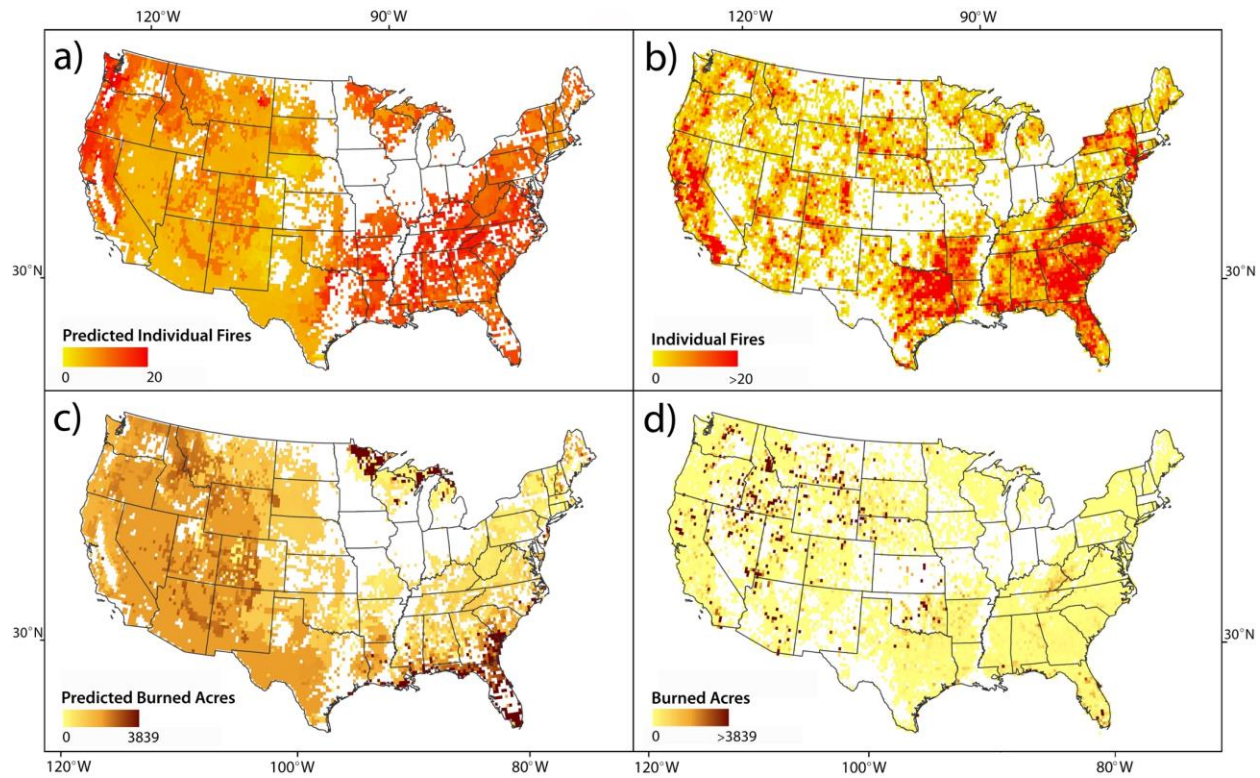
557

558

559

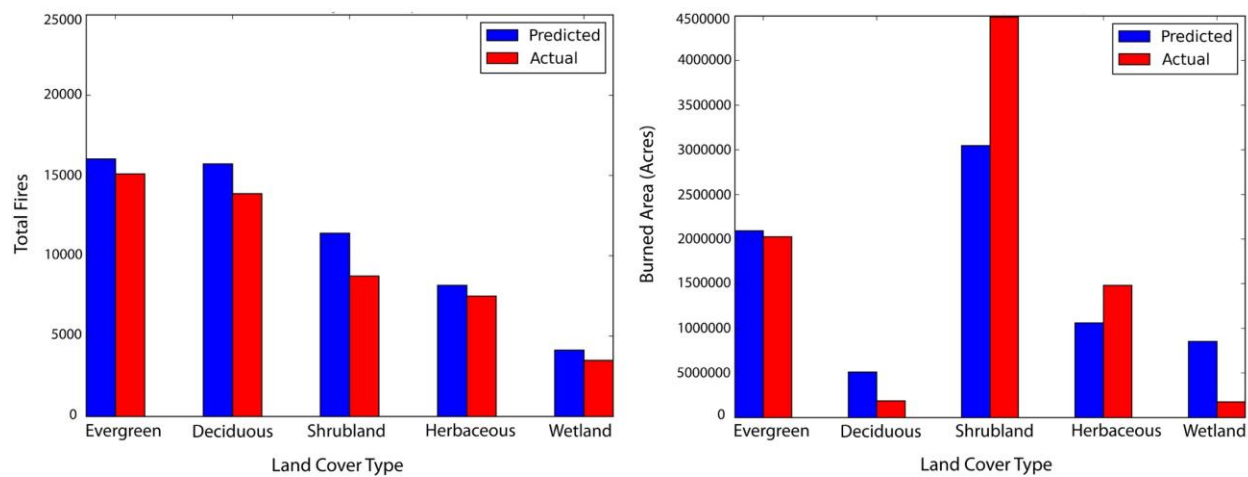
560





549  
550 **Figure 3.** Predictive maps for (a) individual fires and (c) burned area to assess fire risk and  
551 potential from May 2012 – April 2013. These predictive results are compared against the (b) actual  
552 fire distribution and (d) actual burned area for that year for validation.  
553

554



555

556

**Figure 4.** Validation of total predicted fires and burned acres from May 2012 – April 2013.

1  
2  
3  
4  
5  
6  
7  
8  
9  
10  
11  
12  
13  
14  
15  
16  
17  
18  
19  
20  
21  
22  
23  
24  
25  
26  
27  
28  
29  
30  
31  
32  
33  
34  
35  
36  
37  
38  
39  
40  
41  
42  
43  
44  
45  
46  
47  
48  
49  
50  
51  
52  
53  
54  
55  
56  
57  
58  
59  
60